Archives of Endocrinology and Metabolism
ISSN 2359-4292
OFFICIAL JOURNAL OF THE BRAZILIAN SOCIETY OF ENDOCRINOLOGY AND METABOLISM

original

Comprehensive microarray analysis for the identification of therapeutic targets within HIF-1α signalling networks in diet-induced obesity via hypothalamic inflammation

Hai Guo[1,2,3,4,5]
https://orcid.org/0000-0001-7693-9848
Lijuan Ma[2,4,5]
https://orcid.org/0000-0003-1700-9004
Dilihumaier Duolikun[2,4,5]
https://orcid.org/0000-0001-6145-7504
Qiaoling Yao[2,4,5]
https://orcid.org/0000-0002-3379-5263

[1] Department of Anesthesiology, the First Affiliated Hospital of Xinjiang Medical University, Urumqi, Xinjiang, China
[2] Department of Physiology, School of Basic Medical Sciences, Xinjiang Medical University, Urumqi, Xinjiang, China
[3] Xinjiang Perioperative Organ Protection Laboratory (XJDX1411), Urumqi, Xinjiang, China
[4] Xinjiang Key Laboratory of Molecular Biology for Endemic Diseases, Urumqi, Xinjiang, China
[5] State Key Laboratory of Pathogenesis, Prevention and Treatment of High Incidence Diseases in Central Asia, Urumqi, Xinjiang, China

ABSTRACT

Objective: A high-fat diet (HFD) significantly contributes to obesity and alters the neurological function of the brain. This study explored the influence of hypoxia-inducible factor (HIF-1) and its downstream molecules on obesity progression in the context of HFD-induced hypothalamic inflammation. **Materials and methods:** Utilizing a bioinformatics approach alongside animal models, targets and pathways related to hypothalamic obesity were identified via network analysis, gene target identification, gene ontology analysis, Kyoto Encyclopedia of Genes and Genomes (KEGG) pathway enrichment, and subsequent validation in animal models. **Results:** HIF-1α has the potential to regulate the immune response by promoting immune infiltration and increasing the population of immune cells, particularly memory CD4 T cells, in the hypothalamus, primarily through its influence on ksr2 expression. Additionally, the analysis predicted five drugs capable of enhancing HIF-1-Ksr2 signalling. **Conclusion:** In conclusion, targeting Ksr2 with specific drugs represents a potential approach for addressing HFD-induced obesity. These novel findings lay the groundwork for developing dietary supplements and therapeutic interventions.

Keywords: Diet-induced obesity; hypoxia-inducible factor (HIF)-1α; immune infiltration; hypothalamus; ksr2

INTRODUCTION

A high-fat diet (HFD) significantly contributes to obesity and alters neurological function (1). According to previous studies, a high-fat and high-sucrose diet can affect the hypothalamus to regulate the energy balance of the human body (1-3). These factors include hormone production, body temperature regulation, and blood glucose concentration (4,5). A previous study also suggested that dietary obesity was associated with an atypical form of proinflammatory signalling activation leading to background-level inflammation in the hypothalamus (6). This hypothalamus microinflammation may even have the potential to affect the ageing process (7-9). The intricate role of the hypothalamus in maintaining energy balance offers a crucial foundation for addressing obesity.

One potential mechanism underlying HFD-induced hypothalamic inflammation is the presence of saturated fatty acids (SFAs), which can trigger the activation of hypothalamic glial cells, leading to the accumulation of cytokines such as interleukin 1β (IL-1β) and tumour necrosis factor α (TNF-α). This cascade ultimately leads to an inflammatory response (10,11). Another previous study highlighted the ability of hypoxia to increase cholesterol and induce lipid peroxidation, independent of obesity (12). Additionally, the severity of hypoxia determines the degree of metabolic disruption. The reliance of neuronal metabolism on oxygen sensing illustrates how different oxygen levels create diverse metabolic states (13).

Hypoxia-inducible factor (HIF), a dimeric protein composed of a short-life α-subunit and a β

Received on Mar/4/2024
Accepted on Sept/4/2024
DOI: 10.20945/2359-4292-2024-0098

Correspondence to:
Qiaoling Yao
Department of Physiology, School of Basic Medical Sciences, Xinjiang Medical University, No.397, Xinyi Street, Urumqi 830011, China
ql.yao@hotmail.com

constitutively expressed subunit, is the major transcription factor that regulates gene expression in response to hypoxia by inducing or suppressing genes (14). HIF-α is classified into three subtypes: HIF-1α, HIF-2α, and HIF-3α (15,16). HIF-1α plays a critical role in weight regulation, liver metabolism, cardiac metabolism, cancer metabolism, amino acid metabolism, and glucose homeostasis (17-21). Recently, some studies on appetite control in the brain have shown that HIF-1α is highly expressed in the hypothalamus in mice with morbid obesity (22). Some obesity-related genes regulated by HIF-1α also regulate energy metabolism (19). Furthermore, HIF-1α expression and stability increase in the hypothalamus of a HFD-induced obese mouse model (19).

Therefore, the aim of this study was to explore how HIF-1 and its downstream components contribute to obesity amidst hypothalamic inflammation caused by a HFD. We also aimed to propose potential drugs targeting HIF pathways and associated genes to combat HFD-induced obesity.

METHODS

Ethics statement

This study was performed in compliance with the Ethics Guidelines of Animal Fairwell and Care and approved by the institutional animal care review committee of the Animal Experimental Ethical Inspection Committee of the Laboratory Animal Centre, Xinjiang Medical University (No. 2015004). This study followed the Guide for the Care and Use of Laboratory Animals.

Microarray data

GEO, a public genomics repository (http://www.ncbi.nlm.nih.gov/geo), provides extensive gene expression data through microarrays (23). The series matrix files and data table header descriptions of GSE127056 (24) and GSE104709 (25) in the GEO were downloaded to screen and validate genes expressed in the mouse hypothalamus. The GSE127056 dataset, which utilizes the GPL6246 (Affymetrix Mouse Gene 1.0 ST Array) platform, encompasses six samples from HFD-fed mice and three from those fed a normal diet, all from the hypothalamus. The GSE104709 platform, which uses the GPL21103 platform (Illumina HiSeq 4000 for *Mus musculus*), consists of five samples from mice fed a HFD and five from those fed a normal diet. The Combat algorithm of the SVA package (26) in R software (version 4.1.2) was used to eliminate chip batch effects, enabling the exploration of distinct molecular mechanisms between the sample groups. The limma package (27) in R software was used to detect genes with differential expression between the control on a normal diet and the HFD-fed groups, employing a significance threshold of $P < 0.05$ for screening. R's heatmap package generated the heatmap for differentially expressed genes, whereas the ggplot2 package facilitated volcano plot analysis via the same software.

Functional analysis of differentially expressed genes

Gene Ontology (GO) and Kyoto Encyclopedia of Genes and Genomes (KEGG) analyses were used to assess the related available categories. The significant categories included GO- and KEGG-enriched pathways with p values and q values < 0.05. The ssGSEA algorithm (28) was used to quantify the metabolic levels of the DEGs across all the samples, visualizing metabolic pathways through a heatmap.

WGCNA

The R WGCNA package was used to explore coexpression relationships among differentially expressed genes (29). We used the WGCNA-R package, with a soft threshold of 10, to construct coexpression networks of the DEGs. This method converts the weighted adjacency matrix to a topological overlap matrix (TOM), estimating network connections. Hierarchical clustering was used to identify gene modules displayed in distinct colours, organizing genes by shared expression patterns and revealing their interactions.

Immune microenvironment network analysis

CIBERSORT (30) employs support vector regression to deconvolve immune cell subtypes from an expression matrix. It includes 547 biomarkers distinguishing 25 phenotypes of murine immune cells, encompassing T, B, plasma, and myeloid subsets. CIBERSORT was used to analyse the sample data, inferring the relative

proportions of 25 immune-infiltrating cells. A Pearson correlation analysis between gene expression and immune cell content was conducted, and the results were visualized via ggplot2.

GSEA analyses

Gene set enrichment analysis (GSEA; Broad Institute, Inc., Massachusetts Institute of Technology, and University of California Reagents) was used to detect significant expression differences within defined gene sets between two groups (31). The database for annotation, visualization, and integrated discovery [DAVID 6.8 http://david.ncifcrf.gov; (32,33)], an online bioinformatics resource, systematically annotates genes and proteins via diverse biological data. GSEA was used to examine signalling pathways among the high- and low-HIF-1-related gene groups, revealing potential molecular variances. The analysis ranked genes and evaluated enrichment within predefined sets, elucidating molecular differences between sample groups, using a limit of 1,000 substitutions and phenotype definitions.

Transcription regulation analysis

CistromeDB (34) is a vast repository housing 30,451 human and 26,013 mouse ChIP-seq and DNase-seq samples. We explored the regulatory links between transcription factors and key genes via the Cistrome DB, which aligns with mm10 and a 10-kb range around the transcription start site. Visualization of the data was performed via Cytoscape (35).

Animal experiments

Male HIF-1$\alpha^{flox/flox}$ mice bred at Xinjiang Medical University from the Polotsky Laboratory stock (Johns Hopkins University) were housed under controlled SPF-grade conditions. After surgical viral injections with AAV-hSyn-GFP and AAV-hSyn-cre-GFP viruses into the hypothalamic base, the mice were split into two groups: control (AAV-hSyn-GFP) and HIF1αKOMBH (AAV-hSyn-cre-GFP). Daily monitoring of body weight and food intake began on the 5th day postinjection and continued until the 28th day, which was the fourth week after virus administration.

Energy metabolism and behaviour monitoring of the mice

A Promethion animal metabolism and behaviour monitoring system (Sable Systems International, USA) was utilized to measure energy metabolism-related parameters in the mice. This system enables real-time monitoring of mouse energy expenditure and can measure several key indicators, including mouse activity level, oxygen consumption (VO_2), carbon dioxide production (VCO_2), and energy expenditure (EE). The formula for calculating EE is as follows: 3.941 × VO_2 (litres/day) + 1.106 × VCO_2 (litres/day).

The monitoring procedure was as follows: control and HIF1αKOMBH mice 30 days after viral infection were separately placed in individual monitoring chambers equipped with bedding material, where 50 g of food and 100 mL of drinking water were provided. The first 48 hours after the mice were placed in the monitoring chambers were designated the adaptation phase, during which no data collection occurred. After the adaptation period, the system began automatically collecting data on mouse activity, VO_2, and other parameters every 5 minutes, which were continuously recorded for 24 hours. The metabolic chambers were maintained under standard light-dark cycles (lights on at 8:00 AM, off at 8:00 PM) and at a constant temperature of 24 °C.

Histological staining of mouse epididymal fat and scapular brown adipose tissue

The mice were fasted for 6 hours, anaesthetized, and rapidly perfused with sterile physiological saline and 4% paraformaldehyde four weeks after virus injection. Brown adipose tissue from the scapular region and epididymal fat tissue (0.5*0.5 cm) were collected. The tissue blocks were removed from the fixation solution and washed twice with PBS. The fixed tissue blocks underwent gradient ethanol dehydration, transparency, embedding in paraffin, paraffin section preparation, deparaffinization, haematoxylin, and eosin (HE) staining, and sealing on slides with neutral mounting medium. A light microscope and image acquisition system were used to observe and record the morphology of the adipose tissue cells. ImageJ was used to calculate the average cell size in the captured slide images.

Gene expression patterns in the hypothalamus

Hypothalamus tissue was collected and processed for gene expression analysis. RNA was extracted via TRIzol® reagent, reverse-transcribed into cDNA via random primers, and then assessed for selected gene expression via qPCR via designed primers from Oebiotech (Shanghai, China).

CMAP analysis

The CMAP database of the Broad Institute links genes, small molecules, and diseases via gene expression. It encompasses microarray data before and after treatment with 1309 small-molecule drugs across various cancers, aiding in predicting obesity-specific targeted therapy drugs based on differentially expressed obesity genes.

Statistical analysis

Statistical analysis was performed via the R language (version 4.1.2). All the statistical tests were two-sided, and $p < 0.05$ was considered statistically significant.

RESULTS

Differential gene expression in the hypothalamus of HFD-fed mice

We analysed the GEO datasets GSE127056 and GSE104709 to identify obesity-related differentially expressed genes in the hypothalamus of HFD-fed mice. The dataset included 19 samples (control group, n = 8; HFD group, n = 11). Using the Combat algorithm, chip correction reduced batch effects **(Supplementary Figure 1)**. After consolidating and normalizing the data, Limma identified 1173 DEGs (584 upregulated and 589 downregulated) between the groups **(Figure 1A and B)** under screening conditions of $p < 0.05$.

We conducted enrichment analysis on the DEGs to explore their coexpression relationships. Gene Ontology (GO) enrichment revealed pathways related to protein catabolic processes, purine metabolism, ribose phosphate metabolism, and proteasome functions **(Figures 2A)**. KEGG enrichment highlighted pathways such as oxidative phosphorylation and adipocytokine signalling, among others **(Figure 2B)**. Additionally, the metabolic pathway heatmap revealed elevated scores for amino acid metabolism in the HFD samples but lower scores for drug metabolism and other metabolic categories than in the normal samples **(Figure 2C)**.

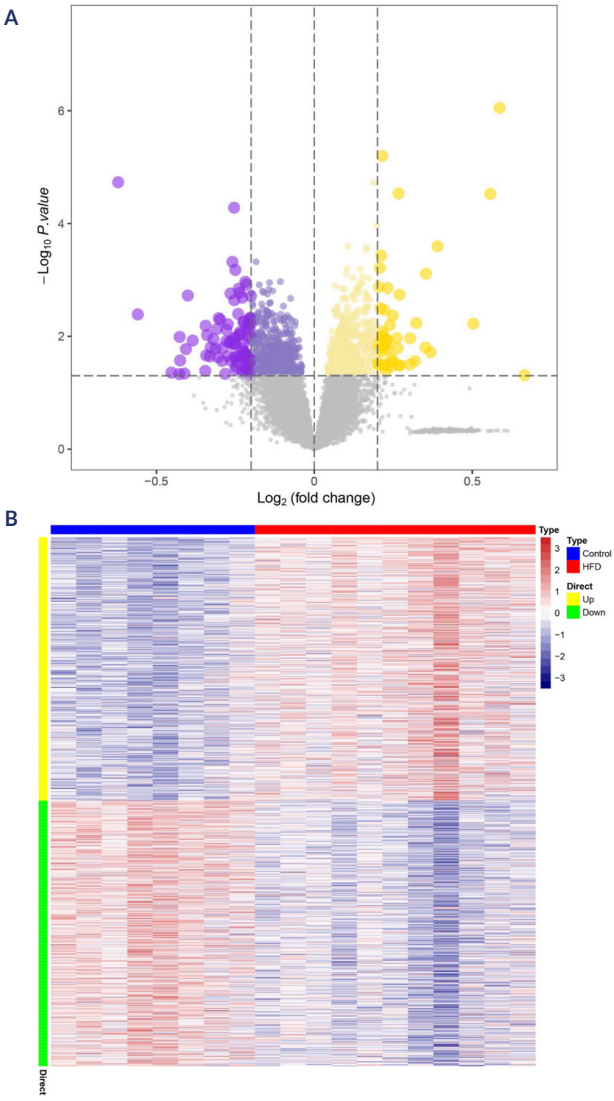

Figure 1. Genome-wide analysis of the hypothalamus of HFD-fed mice. The series matrix files of GSE127056 and GSE104709 were downloaded from the GEO database to screen and verify genes expressed in the mouse hypothalamus. **(A)** Volcano plot analysis was used to identify differentially expressed genes. The yellow and purple dots represent upregulated and downregulated genes, respectively, in the hypothalamus tissue from the HFD groups compared with the normal controls. **(B)** Heatmap of 1173 differentially expressed genes screened by the limma package. Red areas represent highly expressed genes, and blue areas represent genes expressed at low levels in hypothalamus tissue from HFD groups compared with normal controls. HFD: high-fat diet.

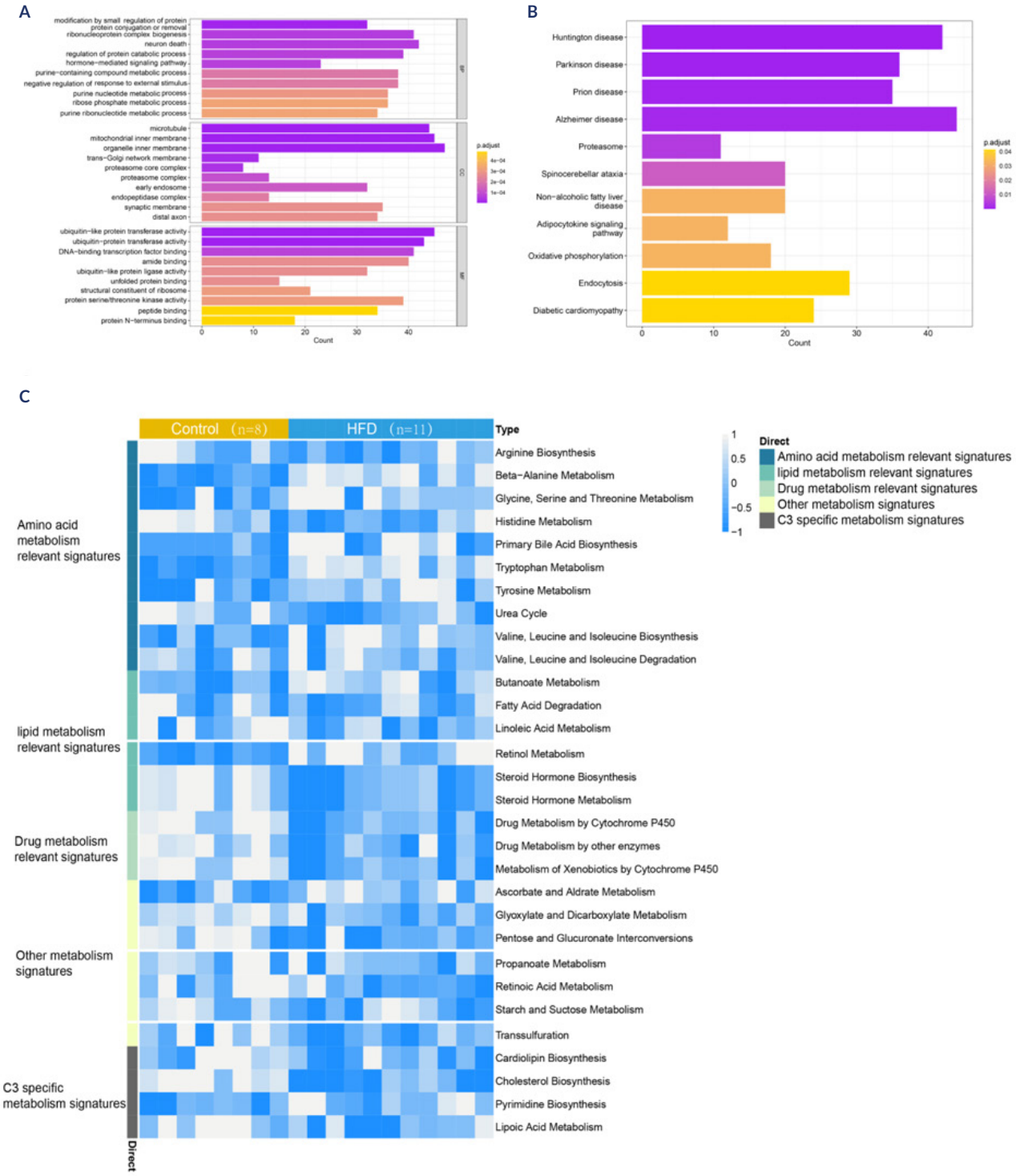

Figure 2. GO and KEGG pathway enrichment analyses of the hypothalamus of HFD-fed mice. The series matrix files of GSE127056 and GSE104709 were downloaded from the GEO database. **(A)** Top 10 gene ontology (GO) terms associated with the biological process (BP), cellular component (CC), and molecular function (MF) categories. **(B)** Target KEGG pathway network of differentially expressed genes. **(C)** Heatmap of metabolic pathway enrichment analysis.

Gene sets regulated by HIF-1α in the hypothalamus of HFD-fed mice

We used expression data of differentially expressed genes to construct a WGCNA network, setting the shear height to 8 and the soft threshold to 10 **(Supplementary Figure 2)**. Five gene modules were identified: black (403), yellow (116), brown (466), red (85), and grey (103). An analysis of the relationships

between the modules and traits revealed that the brown module was highly correlated with HIF-1α (cor = 0.58, p = 0.01) **(Supplementary Figure 3)**. To identify genes strongly correlated with HIF-1α in the brown module, we extracted genes with |GS|>0.5 and |MM|>0.8 for further analysis; this revealed six hub genes: Dynlt3, Zfp770, Hadhb, Mcf2l, Clip2, and Ksr2 **(Figure 3)**.

Immune cell expression profile in the hypothalamus of HFD-fed mice

The microenvironment, including immune cells, impacts disease diagnosis and treatment sensitivity. To analyse the role of the hub genes in obesity, we studied their relationship with immune infiltration. **Figures 4A and 4B** display the immune cell proportions and correlations. The number of memory T CD4+ cells notably increased in the HFD-fed samples **(Figure 4C)**. The six genes strongly correlated with the immune cell content **(Supplementary Figure 4)**. Dynlt3 and Zfp770 were negatively correlated with M0 macrophages, neutrophils, and monocytes; Hadhb was inversely correlated with M0 macrophages; Mcf2l was positively correlated with neutrophils and monocytes; and Clip2 was positively correlated with neutrophils. Additionally, HIF-1α was negatively correlated with monocytes and neutrophils, indicating that immune cell infiltration is influenced by these genes.

HIF-1α $^{flox/flox}$ mice showed signs of obesity

Compared with control mice, HIF1αKOMBH mice consumed more food 10 days after virus injection **(Figure 5A)** and displayed notably greater body weights from Day 16 to Day 30 **(Figure 5B)**. Moreover, their body

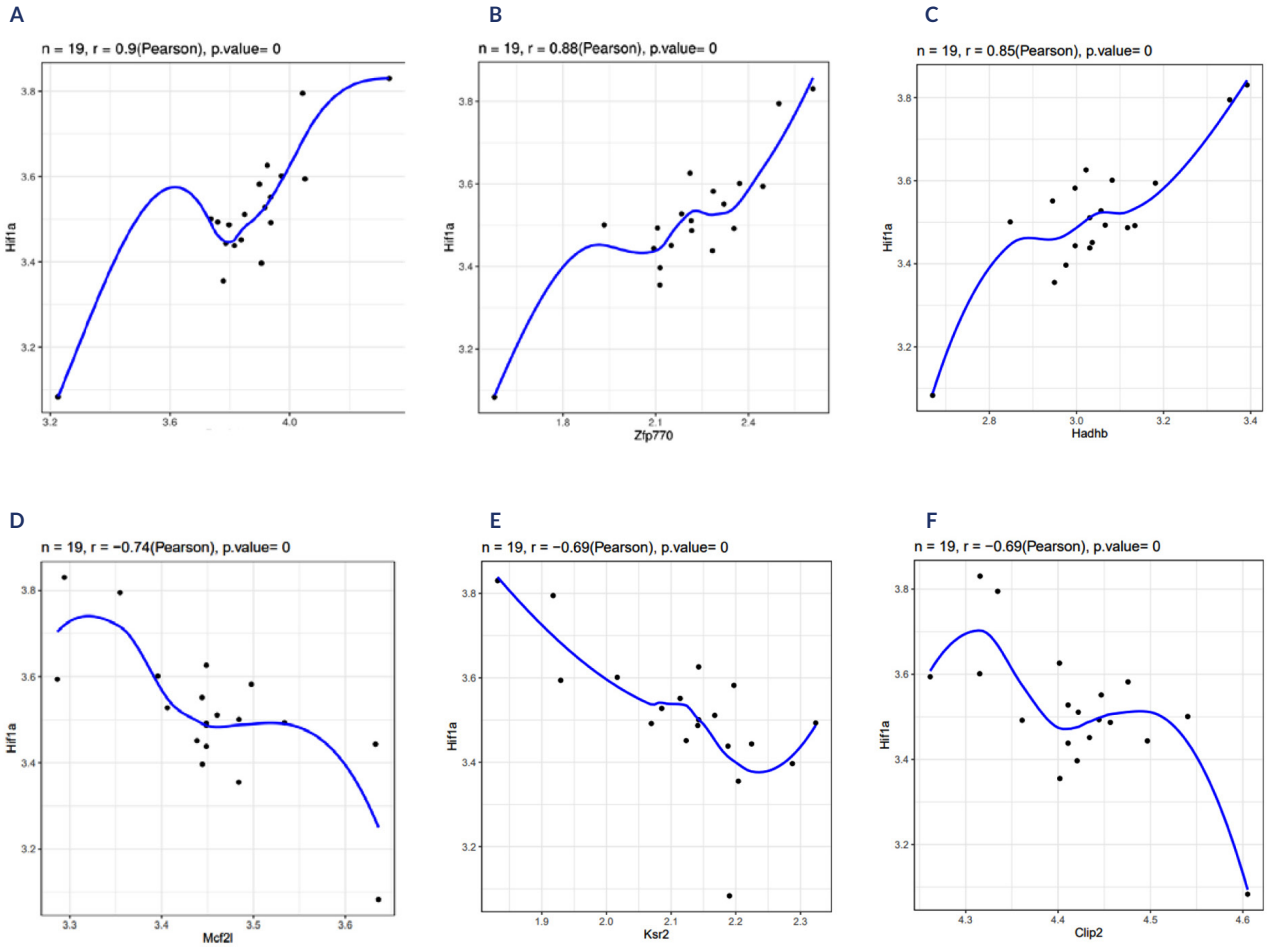

Figure 3. HIF-1α-related hub targets affecting obesity in the hypothalamus of HFD-fed mice. The WGCNA package in R software was used to investigate the coexpression relationship between HIF-1 and differentially expressed genes. **(A)** Dyntl3; **(B)** Zfp770; **(C)** Hadhb; **(D)** Mcf2l; **(E)** Ksr2; **(F)** Clip2.

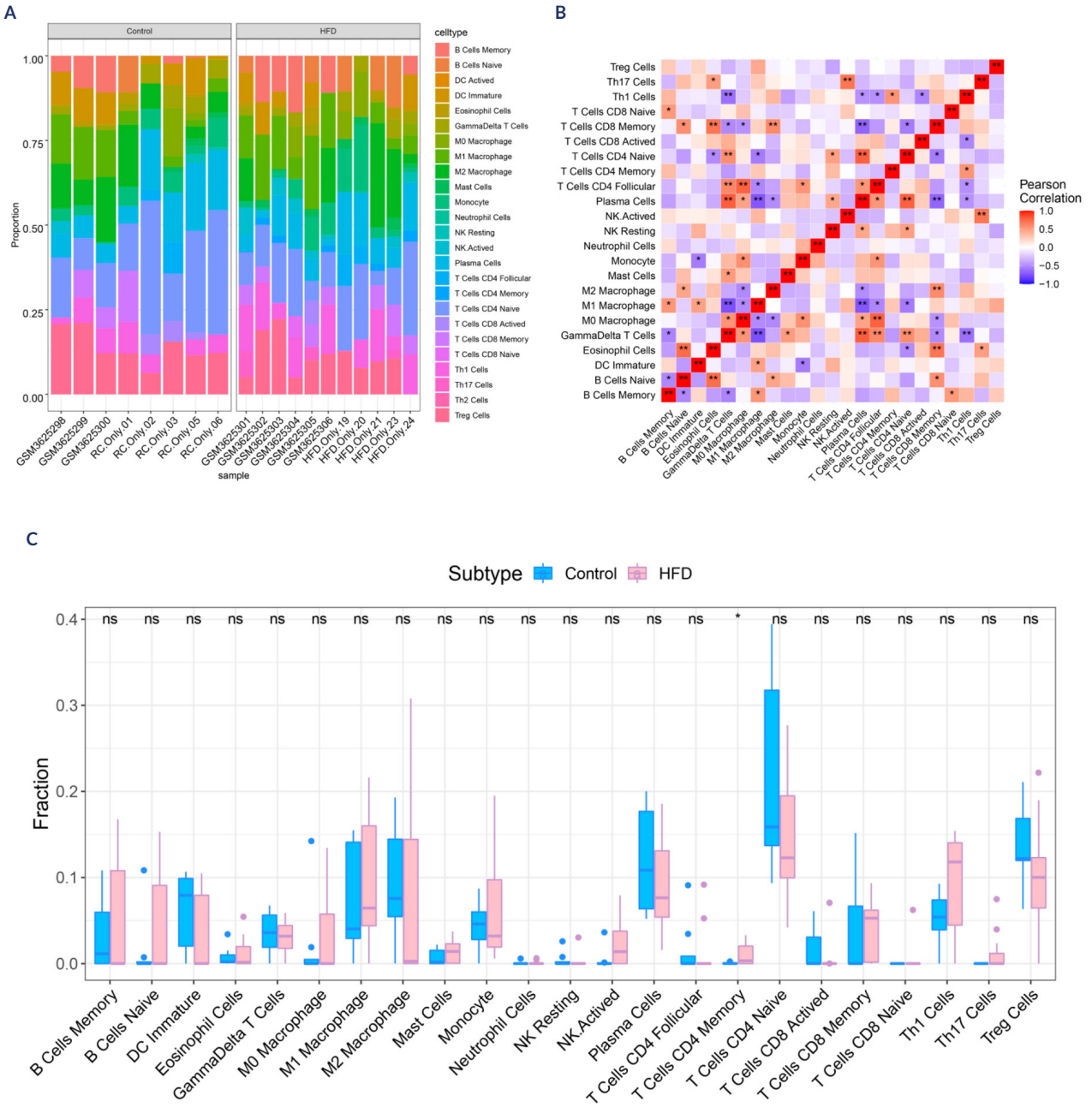

Figure 4. Relationships between the 6 hub genes and immune cell infiltrates in the hypothalamus of HFD-fed mice. The correlation between hub gene expression and resistant cell content was visualized via ggplot2. **(A)** Immune cells contributing to the HFD and control samples. **(B)** Correlations among immune cells. **(C)** The difference in the number of resistant cells between the HFD and control groups. HFD: high-fat diet.

weight gain rate was significantly greater from Day 22 to Day 30 **(Figure 5C)**. Body composition analysis via a live body composition analyser revealed increased fat and body fluid contents in the HIF1αKOMBH group **(Figure 5D)**. The levels of energy metabolism and energy efficiency (EE) in the HIF1αKOMBH group were significantly lower than those in the control group **(Figure 5E)**. HE staining of epididymal fat tissue revealed larger, vacuolated fat cells with increased lipid droplets in the HIF1αKOMBH group **(Figure 5G)**, whereas the control group displayed smaller, densely arranged adipocytes **(Figure 5F)**. Adipocyte area analysis via ImageJ revealed significantly larger adipocyte areas in the HIF1αKOMBH group than in the control group **(Figure 5H)**. Similar findings were observed in brown adipose tissue from the scapular region. The HIF1αKOMBH group presented looser adipose tissue with enlarged cells, reduced cytoplasmic content, and larger lipid droplets **(Figure 5I-5K)**.

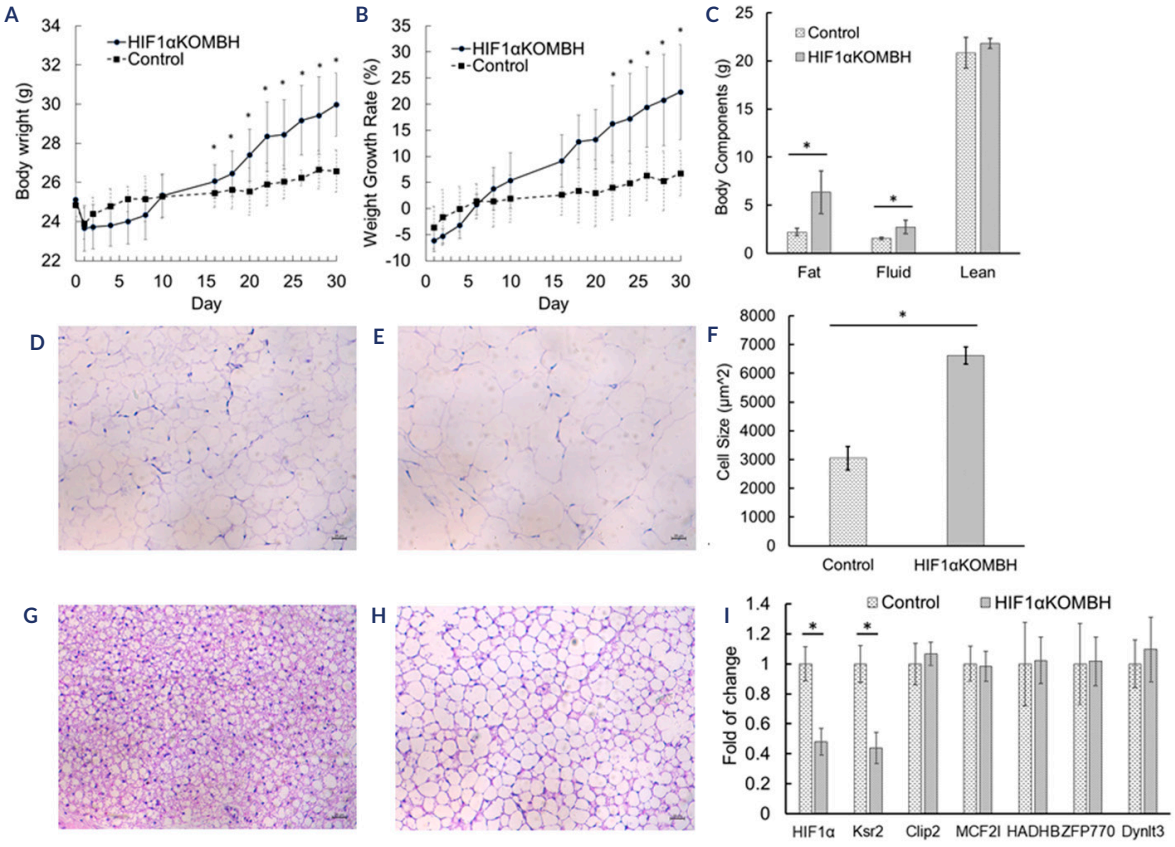

Figure 5. Animal model of HIF-1α $^{flox/flox}$ used in the search for results. In the HIF1aKOMBH group, significant differences were found in the body weights 16 days after virus injection **(B)** and in the weight gain rate 22 days after virus injection **(C)**. The body composition also differed between the two groups **(D)**. The energy efficiency of the HIF1aKOMBH group was significantly lower than that of the control group **(E)**. HE staining of epididymal adipose tissue revealed that the number of cells in the HIF1αKOMBH group **(G)** was significantly greater **(H)** than that in the control group **(F)**. The same phenomena can also be observed in brown adipose tissue **(I-K)**. The qPCR results revealed that the ksr2 gene was the only selected gene underregulated in the hypothalamus of the HIF1αKOMBH group. The scale bars in the images represent 25 μm, and * represents a significant difference **(L)**.

Ksr2 was regulated by HIF-1α in the hypothalamus of HFD-fed mice

Compared with that in the control group, the expression of HIF-1α mRNA in the hypothalamus of HIF-1α$^{flox/flox}$ mice injected with AAV-hSyn-cre-GFP was significantly downregulated by approximately 52% ($P < 0.05$). Additionally, knocking out HIF-1α in the hypothalamic basal nucleus led to a notable reduction in Ksr2 mRNA expression ($P<0.05$). However, the expression of genes such as Dynlt3, Zfp770, Hadhb, Mcf2l, and Clip2 did not significantly differ **(Figure 5I)**.

Novel therapeutic candidates for Ksr2 in obesity-related diseases

Our findings highlight Ksr2 as the sole gene modulated by HIF-1α in the hypothalamus. Using the CMAP database to predict drugs targeting Ksr2, more than 2,000 responses were generated. Given the association of Ksr2 with obesity, drugs capable of upregulating its expression are prioritized. The top five candidates identified were Rho-associated kinase inhibitors, amonafide, phenprobamate, irinotecan, and mitomycin-c **(Table 1 and Figure 6)**.

Table 1. Small-molecule compounds were identified via CMap analysis to reverse the alterations in differentially expressed genes

Rank	Score	Type	ID	Name	Description
20	73.54	cp	BRD-K23875128	RHO-kinase-inhibitor-III [rockout]	Rho-associated kinase inhibitor
24	72.25	cp	BRD-K56334280	amonafide	Topoisomerase inhibitor
25	70.25	cp	BRD-K22009844	phenprobamate	Muscle relaxant
26	69.77	cp	BRD-K08547377	irinotecan	Topoisomerase inhibitor
30	68.44	cp	BRD-A48237631	mitomycin-c	DNA alkylating agent

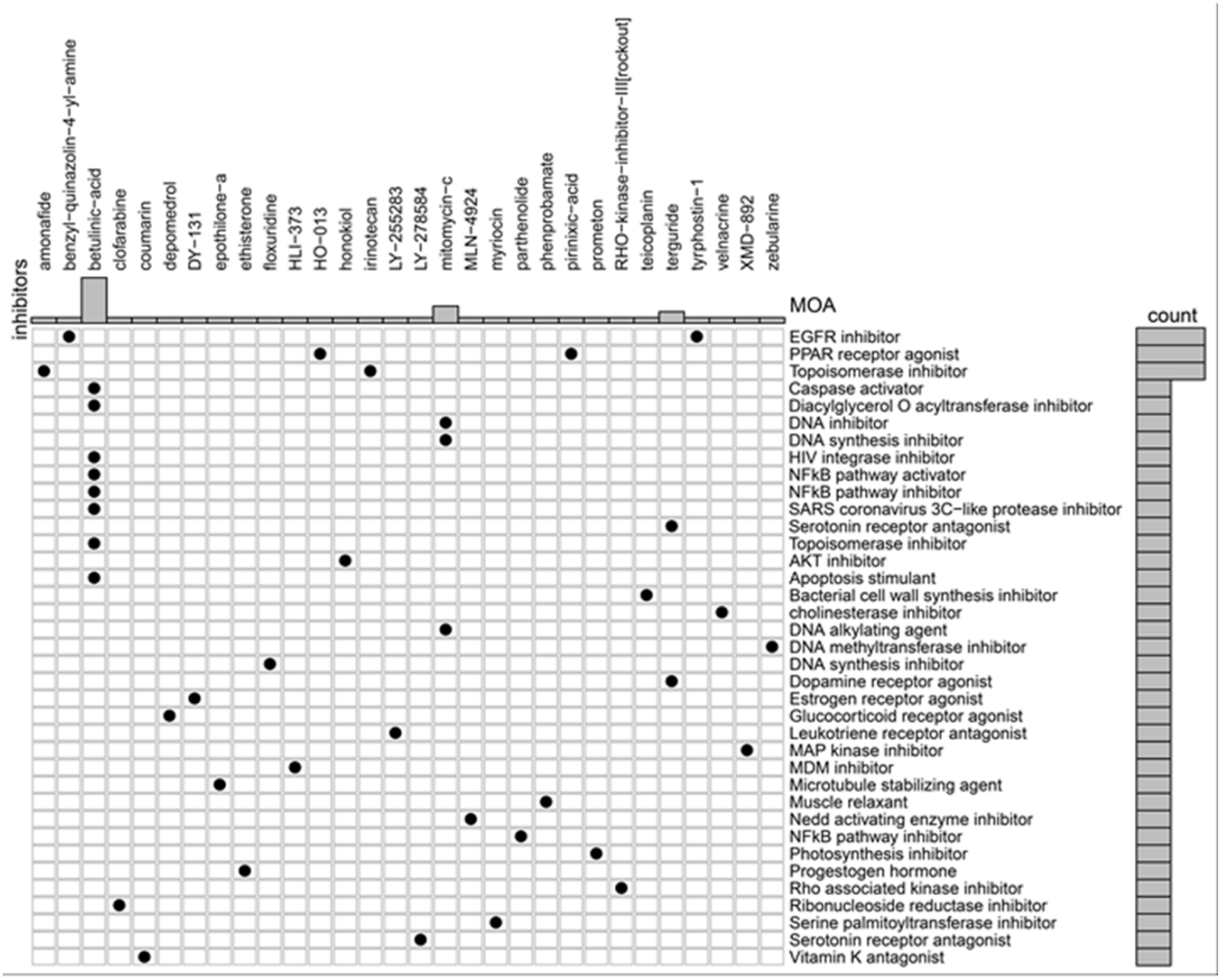

Figure 6. Novel therapeutic targets corresponding to ksr2 genes regulated by HIF-1α in the hypothalamus were predicted via the CMap database. The genes that upregulated ksr2 are shown in the figure.

DISCUSSION

In this study, we employed a bioinformatics approach alongside animal models to explore preventive and therapeutic strategies against HFD-induced obesity. Our results highlight the pivotal role of HIF-1 in orchestrating immune cell infiltration in the hypothalamus, particularly in regulating Ksr2 genes linked to HFD-induced hypothalamic inflammation. Based on these findings, we propose five novel therapeutic candidates aimed at modulating the regulated Ksr2 gene to counteract obesity induced by a HFD.

Louveau and cols. (2015) revealed direct connections between lymphatic vessels and the brain's immune system, underscoring the heightened significance of the immune system within the brain (36). A HFD has been found to trigger hypothalamic inflammation, causing neurological alterations and fostering obesity development. The specialized microglia of the brain, which are unique to the central nervous system, can be influenced by interleukins or chemokines from immune cells, thus regulating inflammatory responses in the brain. Our results revealed that memory CD4+ T-cell counts were markedly greater in the HFD-fed samples than in the regular diet-fed samples. Intriguingly, in the mouse weight regain model, obese mice similarly presented increased memory CD4+ T-cell content. Moreover, our study revealed changes in immune cell expression profiles within the HFD group, affecting M0 macrophages, neutrophils, and monocytes.

These findings establish a link between immune cell infiltration and the HIF-1α pathway in the hypothalamus, suggesting potential approaches for addressing HFD-induced obesity. However, recent research highlights the significant role of the microbiota-gut-brain axis in regulating hypothalamic appetite-related neural networks (37). Specifically, a HFD elevates endocannabinoid levels, alters the gut microbiota composition, and induces endotoxaemia by increasing lipopolysaccharide (LPS) levels; this triggers cytokine-mediated neuroinflammatory responses by compromising the gut and brain barriers (38).

In our animal studies, conditional HIF-1α knockout in the hypothalamus led to obesity even without a HFD. Compared with those in the control group, adipose tissues in the HIF1αKOMBH group presented increased fat content and larger cell size. Additionally, ksr2 gene expression decreased in HIF1αKOMBH mice. KSR2 is an essential intracellular scaffolding protein involved in multiple pathways (39). Previous studies have demonstrated that ksr2-/- mice exhibit obesity, elevated insulin levels, and impaired glucose tolerance (40-43). Furthermore, heterozygous ksr2+/- mice develop obesity when fed a high-fat diet (40). These animal models suggest that KSR2 plays a crucial role in energy homeostasis, insulin sensitivity, and cellular fuel oxidation (40,42).

Further investigations revealed that the function of KSR2 in regulating cellular energy homeostasis is mediated through the activation of 5'-adenosine monophosphate (AMP)-activated protein kinase (AMPK) (44). AMPK is a master regulator of cellular energy homeostasis and senses elevated concentrations of AMP and 5'-adenosine diphosphate (ADP), which are indicative of cellular energy depletion (45,46). By modulating AMPK activity, KSR2 contributes to the maintenance of cellular energy balance and metabolic homeostasis.

These findings suggest that a HFD may initiate hypothalamic inflammation, leading to reduced HIF-1α activity, which subsequently suppresses ksr2 expression, potentially contributing to obesity. Yang and cols. (47) reported a 1.82-fold increase in ksr2 expression in channel catfish under hypoxic conditions, suggesting the potential role of HIF-1α in the upregulation of ksr2. While this evidence is not available for mammals, it implies that HIF-1α could regulate ksr2 expression, supporting the idea that ksr2 expression may decrease when HIF-1α is knocked out in mammalian models.

This study suggested that the ratio of memory CD4+ T cells increases after exposure to a HFD. Upon HFD feeding, perivascular macrophages in the arcuate nucleus of the hypothalamus (ARH) express high levels of inducible nitric oxide synthase, leading to the release of a substantial amount of nitric oxide (NO) (48). NO can inhibit T-cell apoptosis and stimulate the production of recognition molecules on antigen-presenting cells, such as CD1, a lipid-presenting protein. Notably, the activation of CD1-dependent signalling has been associated with increased body mass gain and the exacerbation of diet-induced hypothalamic inflammation (49).

Furthermore, NO stimulates the differentiation and polarization of helper T (Th1) cells through the cyclic guanosine monophosphate (cGMP) pathway (50). While Th1 CD4+ T cells are commonly generated in response to both acute and persistent infections, this population can be lost over time following persistent activation (51). However, NO may help maintain the Th cell population by preventing their apoptosis.

Another mechanism contributing to T-cell memory formation is the activation of the cyclic adenosine monophosphate (cAMP)-protein kinase A signalling pathway, which prevents T-cell death after activation and enhances the generation of memory T cells (52). Interestingly, NO can activate AMP-activated protein kinase (AMPK) by modulating phosphodiesterases (53), which can also modulate the cAMP and cGMP signalling pathways. Given that the kinase suppressor of Ras 2 (KSR2) affects the activity of AMPK, it is plausible that KSR2 may also influence the formation of memory CD4+ T cells. This potential link could be mediated through the modulation of AMPK activity, which in turn affects the cross-talk between the cAMP and cGMP signalling pathways, ultimately impacting T-cell survival and memory formation.

This study, via the CMAP database, identified the top candidates (Rho-associated kinase inhibitors, amonafide, phenprobamate, irinotecan, and mitomycin-C) to increase ksr2 gene activity. Phenprobamate

is a muscle relaxant, while amonafide inhibits topoisomerase I, and irinotecan inhibits topoisomerase II. Mitomycin-C, a DNA alkylating agent, weakens the compact structure of DNA, potentially increasing gene expression by facilitating interactions with the translation machinery. Ksr2 methylation, which is linked to rectal adenocarcinoma survival (54), reveals the role of DNA methylation in compacting DNA and silencing genes, contrasting alkylation effects. These findings underscore the vital epigenetic role of ksr2 in cellular function.

Amonafide and irinotecan, which are potent anticancer drugs, effectively inhibit topoisomerase activity and have been utilized for decades. These drugs inhibit cell proliferation by trapping replication or transcription machinery (55) and induce apoptosis through a ROS-dependent DNA damage signalling pathway (56,57). Camptothecin, a topoisomerase inhibitor, effectively treats obesity in mice by activating glial-derived neurotrophic factor (GDNF) receptor alpha-like (GFRAL) (58). The therapeutic impact of camptothecin mimicked the function of the ksr2 gene, suggesting that similar topoisomerase inhibitors may also prevent obesity.

Stress triggers a complex "fight-or-flight" reaction, releasing hormones such as cortisol into the body (59,60). Prolonged stress can cause muscle tension, resulting in stiffness and discomfort. Muscle relaxants can alleviate this effect by easing contraction. Stress is associated with obesity through various cognitive, behavioural, and physiological mechanisms (61). Stress can impair self-regulation and drive excessive intake of calorie-dense foods; it also triggers the release of hormones such as ghrelin, leptin, and neuropeptide Y, influencing eating behaviour (62-64). Hydralazine, a muscle relaxant, has been shown to reduce body fat by enhancing abdominal subcutaneous adipose tissue lipolysis in both animals and humans (65). These findings suggest that phenprobamate may have a similar effect on weight control and ksr2 stimulation.

Rho-associated kinase inhibitors have emerged as potential treatments for metabolic conditions such as obesity, insulin resistance, dyslipidaemia, and hypertension (66-70). Animal studies suggest that Rho kinase inhibitors positively impact body weight regulation and adipose tissue metabolism (71,72). These inhibitors show promise in reducing food intake, increasing energy expenditure, and impeding fat accumulation and adipocyte differentiation.

While there are limited direct reports confirming the impact of these drugs on obesity, our findings suggest a potential effect of these drugs. Additional animal or randomized clinical studies are crucial to validate or refine our observations.

In conclusion, using a bioinformatics approach alongside animal models, we identified the critical role of HIF-1 in immune cell infiltration within the hypothalamus of HFD-fed mice, linking HFD-induced inflammation to the regulation of the Ksr2 gene through HIF-1. Furthermore, we suggest five potential drugs to target the regulated Ksr2 gene and counter HFD-induced obesity, pending in vitro and in vivo validation for further research.

Consent for publication: all authors approved the manuscript and provided formal written consent to publish the work.

Funding: The study was supported by the State Key Laboratory of Pathogenesis, Prevention and Treatment of Central Asian High Incidence Diseases Fund (SKL-HIDCA-2022-4), and the National Natural Science Foundation of China (81960162).

Acknowledgements: none.

Disclosure: no potential conflict of interest relevant to this article was reported.

REFERENCES

1. Kim JD, Yoon NA, Jin S, Diano S. Microglial UCP2 Mediates Inflammation and Obesity Induced by High-Fat Feeding. Cell Metab. 2019;30(5):952-962.e955. doi: 10.1016/j.cmet.2019.08.010.
2. Brestoff JR, Wilen CB, Moley JR, Li Y, Zou W, Malvin NP, et al. Intercellular Mitochondria Transfer to Macrophages Regulates White Adipose Tissue Homeostasis and Is Impaired in Obesity. Cell Metab. 2021;33(2):270-282.e278. doi: 10.1016/j.cmet.2020.11.008.
3. Varela L, Kim JG, Fernández-Tussy P, Aryal B, Liu ZW, Fernández-Hernando C, et al. Astrocytic lipid metabolism determines susceptibility to diet-induced obesity. Sci Adv. 2021;7(50):eabj2814. doi: 10.1126/sciadv.abj2814.
4. Cakir I, Nillni EA. Endoplasmic Reticulum Stress, the Hypothalamus, and Energy Balance. Trends Endocrinol Metab. 2019;30(3):163-76. doi: 10.1016/j.tem.2019.01.002.
5. Saper CB, Scammell TE, Lu J. Hypothalamic regulation of sleep and circadian rhythms. Nature. 2005;437(7063):1257-63. doi: 10.1038/nature04284.
6. Tang Y, Purkayastha S, Cai D. Hypothalamic microinflammation: a common basis of metabolic syndrome and aging. Trends Neurosci. 2015;38(1):36-44. doi: 10.1016/j.tins.2014.10.002.
7. Bédard K, Bédard J, Rocheleau G, Ferland G, Gaudreau P. Aging and diets regulate the rat anterior pituitary and hypothalamic transcriptome. Neuroendocrinology. 2013;97(2):146-59. doi: 10.1159/000338411.

8. Seong J, Kang JY, Sun JS, Kim KW. Hypothalamic inflammation and obesity: a mechanistic review. Arch Pharm Res. 2019;42(5):383-92. doi: 10.1007/s12272-019-01138-9.
9. Tran DQ, Tse EK, Kim MH, Belsham DD. Diet-induced cellular neuroinflammation in the hypothalamus: Mechanistic insights from investigation of neurons and microglia. Mol Cell Endocrinol. 2016;438:18-26. doi: 10.1016/j.mce.2016.05.015.
10. De Souza CT, Araujo EP, Bordin S, Ashimine R, Zollner RL, Boschero AC, et al. Consumption of a fat-rich diet activates a proinflammatory response and induces insulin resistance in the hypothalamus. Endocrinology. 2005;146(10):4192-9. doi: 10.1210/en.2004-1520.
11. Jais A, Brüning JC. Hypothalamic inflammation in obesity and metabolic disease. J Clin Invest. 2017;127(1):24-32. doi: 10.1172/JCI88878.
12. Cao R, Zhao X, Li S, Zhou H, Chen W, Ren L, et al. Hypoxia induces dysregulation of lipid metabolism in HepG2 cells via activation of HIF-2α. Cell Physiol Biochem. 2014;34(5):1427-41. doi: 10.1159/000366348.
13. Li J, Savransky V, Nanayakkara A, Smith PL, O'Donnell CP, Polotsky VY. Hyperlipidemia and lipid peroxidation are dependent on the severity of chronic intermittent hypoxia. J Appl Physiol (1985). 2007;102(2):557-63. doi: 10.1152/japplphysiol.01081.2006.
14. Cummins EP, Taylor CT. Hypoxia-responsive transcription factors. Pflugers Arch. 2005;450(6):363-71. doi: 10.1007/s00424-005-1413-7.
15. Taylor CT, Colgan SP. Regulation of immunity and inflammation by hypoxia in immunological niches. Nat Rev Immunol. 2017;17(12):774-85. doi: 10.1038/nri.2017.103.
16. Xie C, Yagai T, Luo Y, Liang X, Chen T, Wang Q, et al. Activation of intestinal hypoxia-inducible factor 2a during obesity contributes to hepatic steatosis. Nat Med. 2017;23(11):1298-308. doi: 10.1038/nm.4412.
17. Bouthelier A, Aragones J. Role of the HIF oxygen sensing pathway in cell defense and proliferation through the control of amino acid metabolism. Biochim Biophys Acta Mol Cell Res. 2020;1867(9):118733. doi: 10.1016/j.bbamcr.2020.118733.
18. Courtnay R, Ngo DC, Malik N, Ververis K, Tortorella SM, Karagiannis TC. Cancer metabolism and the Warburg effect: the role of HIF-1 and PI3K. Mol Biol Rep. 2015;42(4):841-51. doi: 10.1007/s11033-015-3858-x.
19. Gaspar JM, Velloso LA. Hypoxia Inducible Factor as a Central Regulator of Metabolism – Implications for the Development of Obesity. Front Neurosci. 2018;12:813. doi: 10.3389/fnins.2018.00813.
20. Knutson AK, Williams AL, Boisvert WA, Shohet RV. HIF in the heart: development, metabolism, ischemia, and atherosclerosis. J Clin Invest. 2021;131(17):e137557. doi: 10.1172/JCI137557.
21. Zhang H, Zhang G, Gonzalez FJ, Park SM, Cai D. Hypoxia-Inducible Factor Directs POMC Gene to Mediate Hypothalamic Glucose Sensing and Energy Balance Regulation. PLoS Biol. 2011;9(7):e1001112. doi: 10.1371/journal.pbio.1001112.
22. Gaspar JM, Mendes NF, Correa-da-Silva F, Lima-Junior JC, Gaspar RC, Ropelle ER, et al. Downregulation of HIF complex in the hypothalamus exacerbates diet-induced obesity. Brain Behav Immun. 2018;73:550-61. doi: 10.1016/j.bbi.2018.06.020.
23. Barrett T, Wilhite SE, Ledoux P, Evangelista C, Kim IF, Tomashevsky M, et al. NCBI GEO: Archive for functional genomics data sets – Update. Nucleic Acids Res. 2013;41(Database issue):D991-5. doi: 10.1093/nar/gks1193.
24. Vagena E, Ryu JK, Baeza-Raja B, Walsh NM, Syme C, Day JP, et al. A high-fat diet promotes depression-like behavior in mice by suppressing hypothalamic PKA signaling. Transl Psychiatry. 2019;9(1):141. doi: 10.1038/s41398-019-0470-1.
25. Perron IJ, Keenan BT, Chellappa K, Lahens NF, Yohn NL, Shockley KR, et al. Dietary challenges differentially affect activity and sleep/wake behavior in mus musculus: Isolating independent associations with diet/energy balance and body weight. PLoS One. 2018;13(5):e0196743. doi: 10.1371/journal.pone.0196743.
26. Leek JT, Johnson WE, Parker HS, Jaffe AE, Storey JD. The sva package for removing batch effects and other unwanted variation in high–throughput experiments. Bioinformatics. 2012;28(6):882-3. doi: 10.1093/bioinformatics/bts034.
27. Ritchie ME, Phipson B, Wu D, Hu Y, Law CW, Shi W, et al. Limma powers differential expression analyses for RNA – sequencing and microarray studies. Nucleic Acids Res. 2015;43(7):e47. doi: 10.1093/nar/gkv007.
28. Chong W, Shang L, Liu J, Fang Z, Du F, Wu H, et al. m^{6}A regulator-based methylation modification patterns characterized by distinct tumor microenvironment immune profiles in colon cancer. Theranostics. 2021;11(5):2201-17. doi: 10.7150/thno.52717.
29. Langfelder P, Horvath S. WGCNA: An R package for weighted correlation network analysis. BMC Bioinformatics. 2008;9:559. doi: 10.1186/1471-2105-9-559.
30. Chen B, Khodadoust MS, Liu CL, Newman AM, Alizadeh AA. Profiling Tumor Infiltrating Immune Cells with CIBERSORT. Methods Mol Biol. 2018;1711:243-59. doi: 10.1007/978-1-4939-7493-1_12.
31. Subramanian A, Tamayo P, Mootha VK, Mukherjee S, Ebert BL, Gillette MA, et al. Gene set enrichment analysis: A knowledge–based approach for interpreting genome–wide expression profiles. Proc Natl Acad Sci U S A. 2005;102(43):15545-50. doi: 10.1073/pnas.0506580102.
32. Huang DW, Sherman BT, Lempicki RA. Bioinformatics enrichment tools: Paths toward the comprehensive functional analysis of large gene lists. Nucleic Acids Res. 2009;37(1):1-13. doi: 10.1093/nar/gkn923.
33. Huang DW, Sherman BT, Lempicki RA. Systematic and integrative analysis of large gene lists using DAVID bioinformatics resources. Nat Protoc. 2009;4(1):44-57. doi: 10.1038/nprot.2008.211.
34. Zheng R, Wan C, Mei S, Qin Q, Wu Q, Sun H, et al. Cistrome Data Browser: expanded datasets and new tools for gene regulatory analysis. Nucleic Acids Res. 2019;47(D1):D729-35. doi: 10.1093/nar/gky1094.
35. Shannon P, Markiel A, Ozier O, Baliga NS, Wang JT, Ramage D, et al. Cytoscape: a software environment for integrated models of biomolecular interaction networks. Genome Res. 2003;13(11):2498-504. doi: 10.1101/gr.1239303.
36. Louveau A, Smirnov I, Keyes TJ, Eccles JD, Rouhani SJ, Peske JD, et al. Structural and functional features of central nervous system lymphatic vessels. Nature. 2015;523(7560):337-41. doi: 10.1038/nature14432.
37. Forte N, Fernández-Rilo AC, Palomba L, Di Marzo V, Cristino L. Obesity Affects the Microbiota-Gut-Brain Axis and the Regulation Thereof by Endocannabinoids and Related Mediators. Int J Mol Sci. 2020;21(5):1554. doi: 10.3390/ijms21051554.
38. Salas-Venegas V, Flores-Torres RP, Rodríguez-Cortés YM, Rodríguez-Retana D, Ramírez-Carreto RJ, Concepción-Carrillo LE, et al. The Obese Brain: Mechanisms of Systemic and Local Inflammation, and Interventions to Reverse the Cognitive Deficit. Front Integr Neurosci. 2022;16:798995. doi: 10.3389/fnint.2022.798995.
39. Pearce LR, Atanassova N, Banton MC, Bottomley B, van der Klaauw AA, Revelli JP, et al. KSR2 Mutations Are Associated with Obesity, Insulin Resistance, and Impaired Cellular Fuel Oxidation. Cell. 2013;155(4):765-77. doi: 10.1016/j.cell.2013.09.058.
40. Revelli JP, Smith D, Allen J, Jeter-Jones S, Shadoan MK, Desai U, et al. Profound obesity secondary to hyperphagia in mice lacking kinase suppressor of ras 2. Obesity (Silver Spring). 2011;19(5):1010-8. doi: 10.1038/oby.2010.282.
41. Brommage R, Desai U, Revelli JP, Donoviel DB, Fontenot GK, Dacosta CM, et al. High-throughput screening of mouse knockout lines identifies true lean and obese phenotypes. Obesity (Silver Spring). 2008;16(10):2362-7. doi: 10.1038/oby.2008.361.
42. Costanzo-Garvey DL, Pfluger PT, Dougherty MK, Stock JL, Boehm M, Chaika O, et al. KSR2 is an essential regulator of AMP kinase, energy expenditure, and insulin sensitivity. Cell Metab. 2009;10(5):366-78. doi: 10.1016/j.cmet.2009.09.010.

43. Guo L, Costanzo-Garvey DL, Smith DR, Neilsen BK, MacDonald RG, Lewis RE. Kinase Suppressor of Ras 2 (KSR2) expression in the brain regulates energy balance and glucose homeostasis. Mol Metab. 2016;6(2):194-205. doi: 10.1016/j.molmet.2016.12.004.
44. Fernandez MR, Henry MD, Lewis RE. Kinase suppressor of Ras 2 (KSR2) regulates tumor cell transformation via AMPK. Mol Cell Biol. 2012;32(18):3718-31. doi: 10.1128/MCB.06754-11.
45. Hardie DG. AMP-activated protein kinase: an energy sensor that regulates all aspects of cell function. Genes Dev. 2011;25(18):1895-908. doi: 10.1101/gad.17420111.
46. Garcia D, Shaw RJ. AMPK: Mechanisms of Cellular Energy Sensing and Restoration of Metabolic Balance. Mol Cell. 2017;66(6):789-800. doi: 10.1016/j.molcel.2017.05.032.
47. Yang Y, Fu Q, Wang X, Liu Y, Zeng Q, Li Y, et al. Comparative transcriptome analysis of the swimbladder reveals expression signatures in response to low oxygen stress in channel catfish, Ictalurus punctatus. Physiol Genomics. 2018;50(8):636-47. doi: 10.1152/physiolgenomics.00125.2017.
48. Lee CH, Suk K, Yu R, Kim MS. Cellular Contributors to Hypothalamic Inflammation in Obesity. Mol Cells. 2020;43(5):431-7. doi: 10.14348/molcells.2020.0055.
49. Bombassaro B, Ramalho AFS, Fioravante M, Solon C, Nogueira G, Nogueira PAS, et al. CD1 is involved in diet-induced hypothalamic inflammation in obesity. Brain Behav Immun. 2019;78:78-90. doi: 10.1016/j.bbi.2019.01.011.
50. Gnipp S, Mergia E, Puschkarow M, Bufe A, Koesling D, Peters M. Nitric oxide dependent signaling via cyclic GMP in dendritic cells regulates migration and T-cell polarization. Sci Rep. 2018;8(1):10969. doi: 10.1038/s41598-018-29287-9.
51. Snell LM, Osokine I, Yamada DH, De La Fuente JR, Elsaesser HJ, Brooks DG. Overcoming CD4 Th1 cell fate restrictions to sustain antiviral CD8 T cells and control persistent virus infection. Cell Rep. 2016;16:3286-96. doi: 10.1016/j.celrep.2016.08.065.
52. Suresh R, Vig M, Bhatia S, Goodspeed EP, John B, Kandpal U, et al. Pentoxifylline functions as an adjuvant in vivo to enhance T cell immune responses by inhibiting activation-induced death. J Immunol. 2002;169(8):4262-72. doi: 10.4049/jimmunol.169.8.4262.
53. Dillard J, Meng X, Nelin L, Liu Y, Chen B. Nitric oxide activates AMPK by modulating PDE3A in human pulmonary artery smooth muscle cells. Physiol Rep. 2020;8(17):e14559. doi: 10.14814/phy2.14559.
54. Pan X, Yi X, Lan M, Su X, Zhou F, Wu W. Research on the pathological mechanism of rectal adenocarcinoma based on DNA methylation. Medicine (Baltimore). 2023;102(4):e32763. doi: 10.1097/MD.0000000000032763.
55. Mabb AM, Simon JM, King IF, Lee HM, An LK, Philpot BD, et al. Topoisomerase 1 Regulates Gene Expression in Neurons through Cleavage Complex-Dependent and -Independent Mechanisms. PLoS One. 2016;11(5):e0156439. doi: 10.1371/journal.pone.0156439.
56. Jang JY, Kang YJ, Sung B, Kim MJ, Park C, Kang D, et al. MHY440, a Novel Topoisomerase I Inhibitor, Induces Cell Cycle Arrest and Apoptosis via a ROS-Dependent DNA Damage Signaling Pathway in AGS Human Gastric Cancer Cells. Molecules. 2018;24(1):96. doi: 10.3390/molecules24010096.
57. Liu J, Qu L, Meng L, Shou C. Topoisomerase inhibitors promote cancer cell motility via ROS-mediated activation of JAK2-STAT1-CXCL1 pathway. J Exp Clin Cancer Res. 2019;38(1):370. doi: 10.1186/s13046-019-1353-2.
58. Lu JF, Zhu MQ, Xie BC, Shi XC, Liu H, Zhang RX, et al. Camptothecin effectively treats obesity in mice through GDF15 induction. PLoS Biol. 2022;20(2):e3001517. doi: 10.1371/journal.pbio.3001517.
59. Fogelman N, Canli T. Early life stress and cortisol: A meta-analysis. Horm Behav. 2018;98:63-76. doi: 10.1016/j.yhbeh.2017.12.014.
60. Pulopulos MM, Baeken C, De Raedt R. Cortisol response to stress: The role of expectancy and anticipatory stress regulation. Horm Behav. 2020;117:104587. doi: 10.1016/j.yhbeh.2019.104587.
61. Kumar R, Rizvi MR, Saraswat S. Obesity and Stress: A Contingent Paralysis. Int J Prev Med. 2022;13:95. doi: 10.4103/ijpvm.IJPVM_427_20.
62. Chao AM, Jastreboff AM, White MA, Grilo CM, Sinha R. Stress, cortisol, and other appetite-related hormones: Prospective prediction of 6-month changes in food cravings and weight. Obesity (Silver Spring). 2017;25(4):713-20. doi: 10.1002/oby.21790.
63. Jeanrenaud B, Rohner-Jeanrenaud F. CNS-periphery relationships and body weight homeostasis: influence of the glucocorticoid status. Int J Obes Relat Metab Disord. 2000;24 Suppl 2:S74-6. doi: 10.1038/sj.ijo.0801283.
64. Tomiyama AJ, Schamarek I, Lustig RH, Kirschbaum C, Puterman E, Havel PJ, et al. Leptin concentrations in response to acute stress predict subsequent intake of comfort foods. Physiol Behav. 2012;107(1):34-9. doi: 10.1016/j.physbeh.2012.04.021.
65. Arima H, Oiso Y. Positive effect of baclofen on body weight reduction in obese subjects: a pilot study. Intern Med. 2010;49(19):2043-7. doi: 10.2169/internalmedicine.49.3918.
66. Hara Y, Wakino S, Tanabe Y, Saito M, Tokuyama H, Washida N, et al. Rho and Rho-kinase activity in adipocytes contributes to a vicious cycle in obesity that may involve mechanical stretch. Sci Signal. 2011;4(157):ra3. doi: 10.1126/scisignal.2001227.
67. Jahani V, Kavousi A, Mehri S, Karimi G. Rho kinase, a potential target in the treatment of metabolic syndrome. Biomed Pharmacother. 2018;106:1024-30. doi: 10.1016/j.biopha.2018.07.060.
68. Lee SH, Huang H, Choi K, Lee DH, Shi J, Liu T, et al. ROCK1 isoform-specific deletion reveals a role for diet-induced insulin resistance. Am J Physiol Endocrinol Metab. 2014;306(3):E332-43. doi: 10.1152/ajpendo.00619.2013.
69. Liu L, Tan L, Lai J, Li S, Wang DW. Enhanced Rho-kinase activity: Pathophysiological relevance in type 2 diabetes. Clin Chim Acta. 2016;462:107-10. doi: 10.1016/j.cca.2016.09.003.
70. Liu PY, Chen JH, Lin LJ, Liao JK. Increased Rho kinase activity in a Taiwanese population with metabolic syndrome. J Am Coll Cardiol. 2007;49(15):1619-24. doi: 10.1016/j.jacc.2006.12.043.
71. Noda K, Nakajima S, Godo S, Saito H, Ikeda S, Shimizu T, et al. Rho-kinase inhibition ameliorates metabolic disorders through activation of AMPK pathway in mice. PLoS One. 2014;9(11):e110446. doi: 10.1371/journal.pone.0110446.
72. Wei L, Shi J. Insight into Rho Kinase Isoforms in Obesity and Energy Homeostasis. Front Endocrinol (Lausanne). 2022;13:886534. doi: 10.3389/fendo.2022.886534.

SUPPLEMENTARY

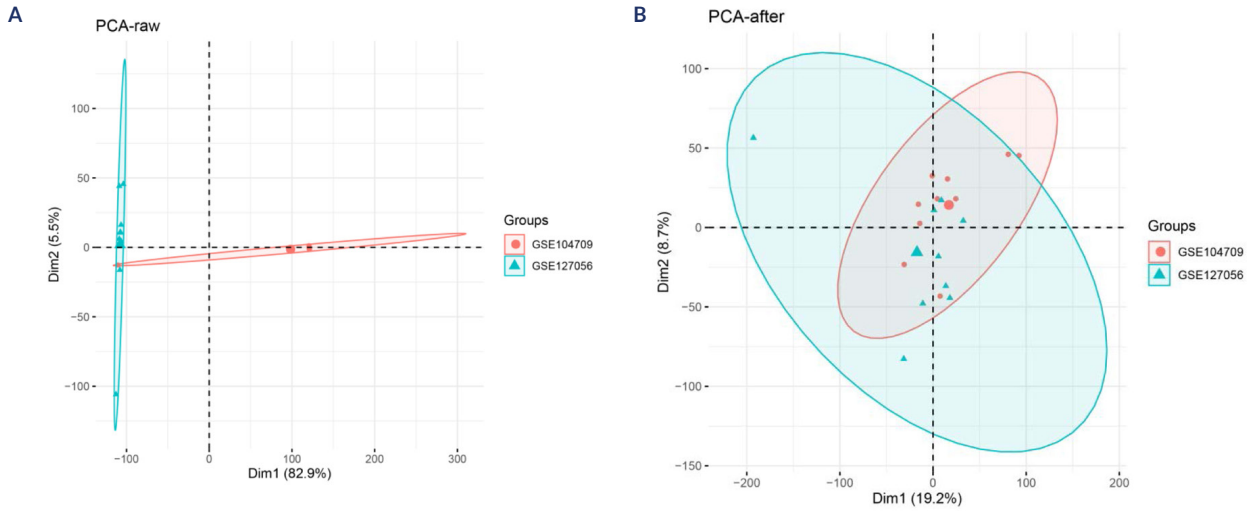

Supplementary Figure 1. The batch effect between chips is reduced after Combat algorithm correction. A plot of principal component analysis (PCA) factors related to obesity was generated from the GEO datasets GSE127056 and GSE104709. (**A**) Before combat algorithm correction. (**B**) After combat algorithm correction.

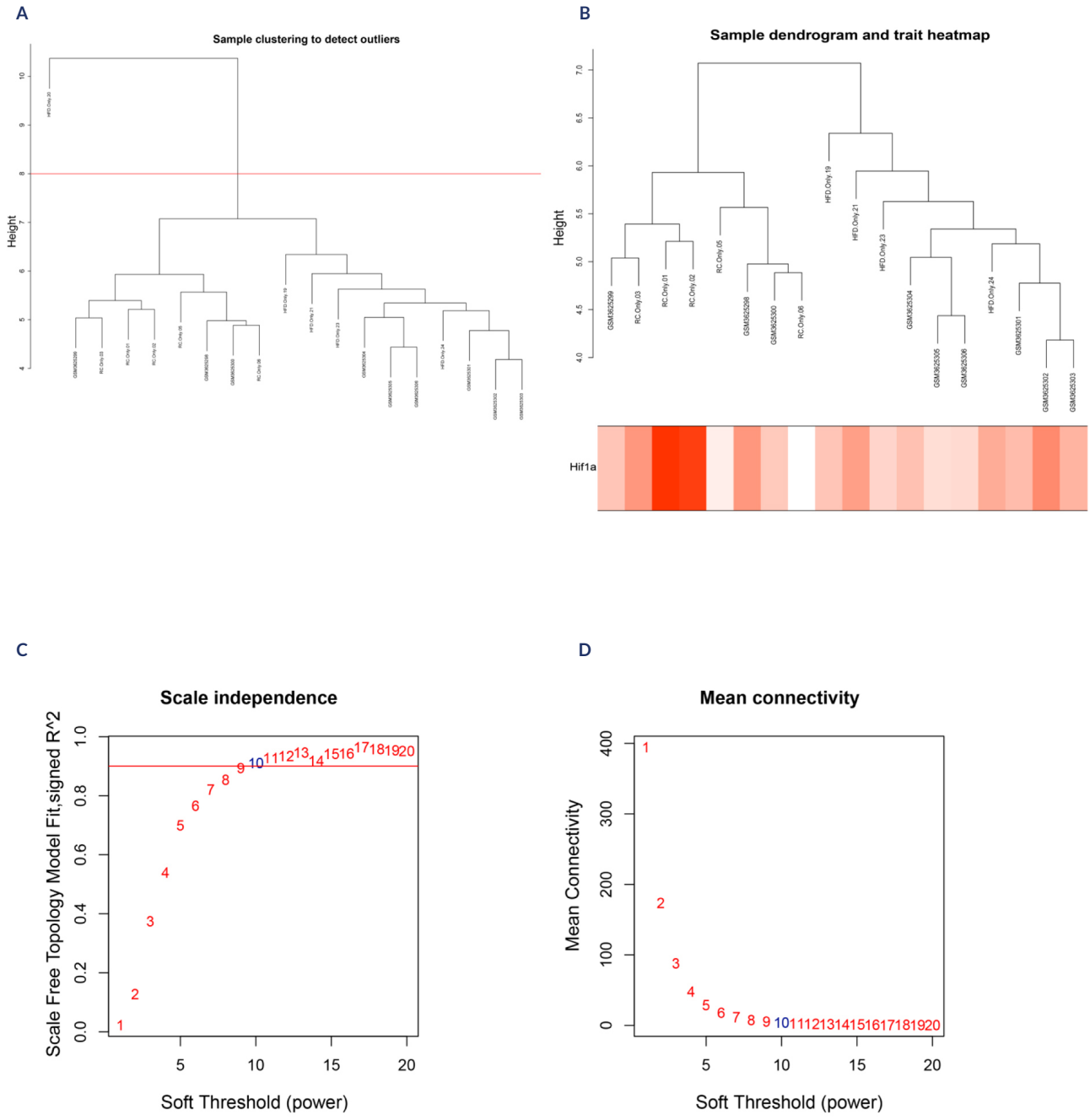

Supplementary Figure 2. The WGCNA network is based on the expression data of differentially expressed genes and was used to explore the HIF-1α-related coexpression network. **(A)** Cluster dendrogram. The red line represents the cut-off of data filtering in the data processing step. **(B)** Sample dendrogram and trait indicators. **(C)** Analysis of the scale-free fit index for various soft-thresholding powers. The red line represents the cut-off value. **(D)** Analysis of the mean connectivity for different soft thresholding powers.

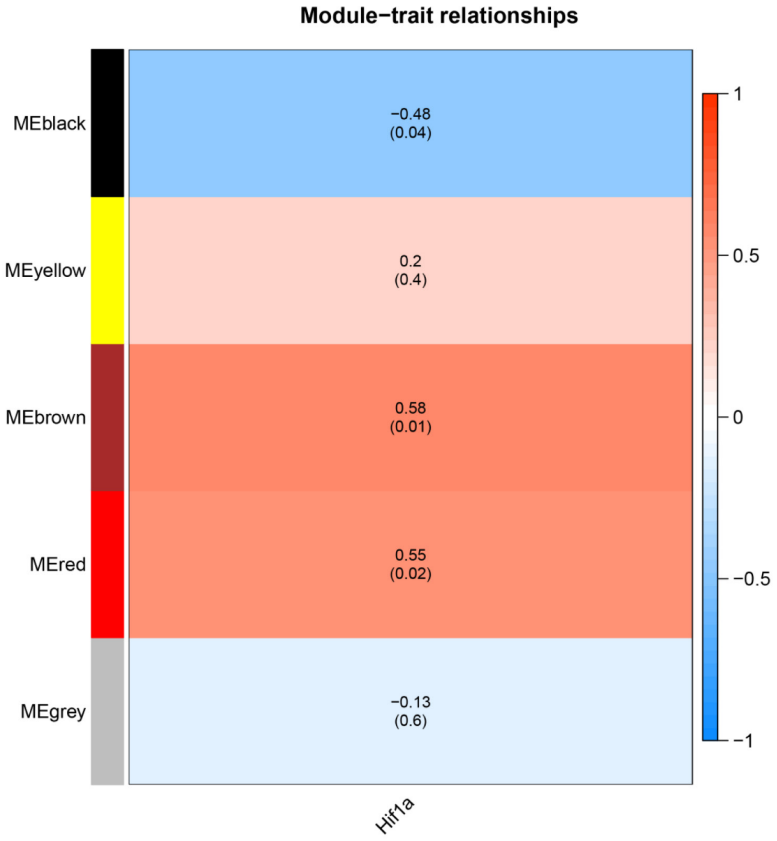

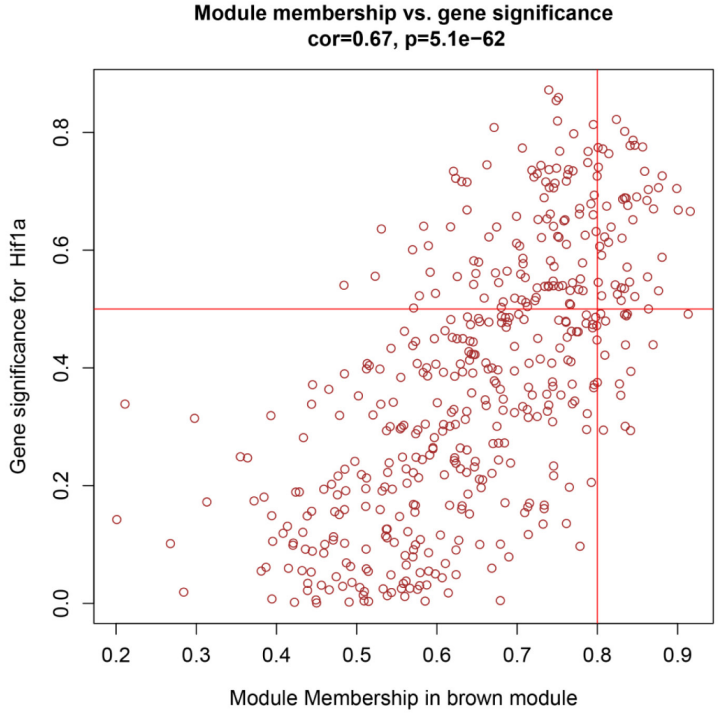

Supplementary Figure 3. Main findings in the module-trait correlation analyses. Heatmap of the correlations between modules and HIF-1α (each gene module contained a correlation coefficient and corresponding p value). The gene significance for HIF-1α in the turquoise module (one dot represents one gene in the turquoise module).

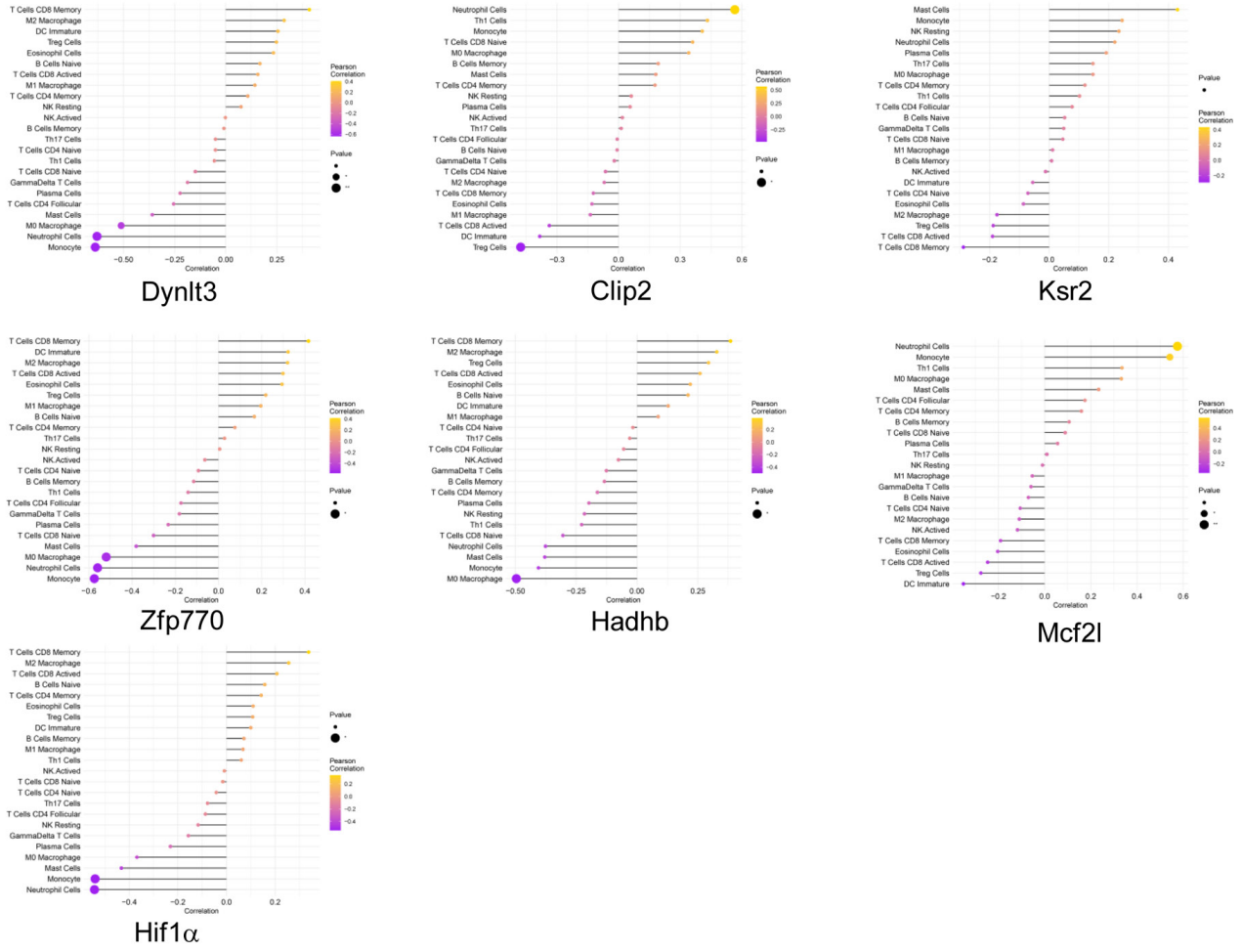

Supplementary Figure 4. Correlations between the 7 genes and immune cells. Correlation matrix of the Pearson correlation coefficients.